LAND SURFACE TEMPERATURE MAPPING BY THE USE OF REMOTE SENSING AND GIS: CASE STUDY OF ISTANBUL METROPOLITAN AREA

İ.Yakar, S.Bilgi*

İTÜ Geomatics Engineering Department, 34485, Maslak-Istanbul, Turkey, (yakari, bilgi)@itu.edu.tr

KEYWORDS: Land Surface Temperature, Thermal Remote Sensing, Geographic Information Systems

ABSTRACT:

Istanbul has faced rapid urban development especially in the last 50 years. This situation caused a significant change in population of the city as well. Thus, land cover type has changed from rural to artificial materials. The surface temperatures were affected by the change in the amount of evaporation and permeability on the soil surface due to the effect of building stock. Since, the land surface temperature affects so many areas such as public health, traffic, environmental health etc., determination of land surface temperature is very essential for future of the city. Along with the developing technology, surface temperatures can be determined using thermal remote sensing. In this study, land surface temperature maps were produced by using Istanbul satellite imagery of different dates on ArcGIS software and differences have been examined in terms of management of green areas, planning of construction studies, development of the city etc.

1. INTRODUCTION

Population growth and economic expansion can be listed as the primary factors that affect the land use and land cover (LULC) change worldwide, especially in developing countries. Although the urban areas constitute 2 % of the earth's surface, it has huge impact on local and global ecosystems. Therefore, it is important to determine the LULC and related issues. In this aspect, highly accurate LULC classification can be conducted by the ground surveys. However, these options are expensive and time-consuming. This situation indicates the importance of remote sensing as an apparent and preferred alternative (Jeevalakshmi et. Al, 2017). On the other hand, land surface temperature (LST) can be shown as one of the most affected factors by urban changes related with the human activities (Lv and Zhou,2011). In this context, remote sensing is a useful discipline for LST estimation. The distribution of thermal phenomenon basically refers to differences between various land use and land cover types. Typically, the densely built areas have higher temperature values compared with the surrounding rural areas. With the developing technology, the sensors specially designed for the thermal remote sensing have an important role on the studies related with the LST estimation. Researches on LST estimation indicates that the conversion of surface soil, water content and vegetation can be highly effective on the balance of land surface energy. In general, LST is a result of the different surface properties such as albedo, emissivity and thermal properties of land cover types. Each of these parameters results in wide range of variations with the land use and land cover change caused by the rapid urbanization (Lv and Zhou,2011). Different methods have been developed for obtaining the LST by the use of thermal infrared (TIR) data (Li and Duan, 2017). In this study, the land surface temperature maps are obtained by the use of two Landsat 5 satellite images respectively acquired on 3 March 1999 and 3 May 2010 and one Landsat 8 image acquired on 25 March 2019 were used for land surface temperature estimation. The inversion of Planck's Function is conducted on the ESRI ArcGIS 10.4 software for LST estimation. The details of the study and case study will be mentioned in the related sections. It is seen that the temperature of the study area has significantly changed from 1999 to 2019. The comparison specifically has been done at a specific season to indicate the seasonal differences. It is also seen that the built-up areas and bare lands have relatively higher temperature values than the surrounding areas.

2. STUDY AREA and DATA

2.1 Study Area

Istanbul city which has faced rapid urban development and population growth especially in past 70 years, has been chosen as the study area. The city is located between at 40˚58' N latitude and 28˚50' E longitude in Turkey (Figure 1). Its population was nearly 3 million in 1970s while it has reached around 15 million today. On the other hand, unplanned urban expansion in the city resulted in significant land cover changes. Since this situation affects wide range of areas such as public health, environmental health, traffic etc., determination of LST plays an important role on sustainable development of the city.

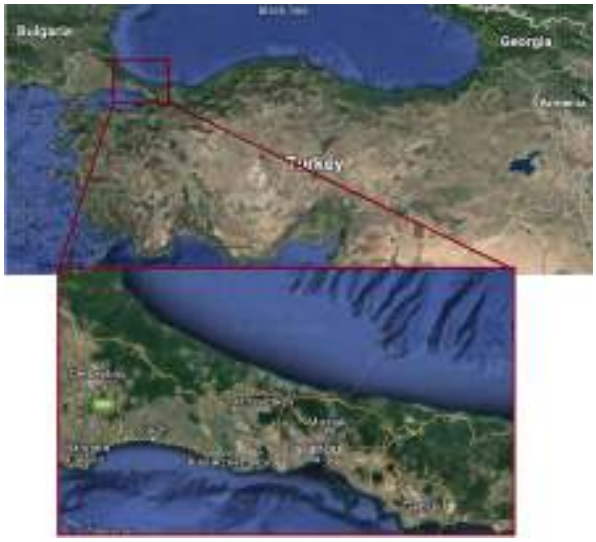

Figure 1: Study area **(Google Earth, 2019)**

2.2 Data

In this study**,** Landsat 8 Operational Land Imager & Thermal Infrared Sensors (OLI & TIRS) data acquired on March 25, 2019 and two Landsat 5 data respectively acquired on March 2, 1999 and May 3, 2010 were used. Acquiring dates and sensors of the images are shown in Table 3. The data used in this study are obtained from USGS's Earth Explorer. Landsat 8 contains two sensors such as the Operational Land Imager (OLI) and the Thermal Infrared Sensor (TIRS) and launched on February 11, 2013 (Landsat Science, 2019). It contains two thermal infrared bands which are band 10 and band 11. In addition, Landsat 5 launched on March 1, 1984. It consists of 6 bands with a spatial resolution of 30 meters and one thermal infrared band with a resolution of 120 meters (USGS,n.d.). The properties of Landsat 4-5 TM and Landsat 8 OLI & TIRS are shown in the tables (1) and (2) respectively. In the estimation of land surface temperature, the thermal infrared bands of Landsat 8 OLI & TIRS (Band 10) and Landsat 5 TM (Band 6) were used. In addition, Normalized Difference Vegetation Index (NDVI) values were obtained by the use of near infrared (NIR) and red bands.

Landsat 4-5 TM Bands		
Spatial Resolution	Wavelength (micrometers)	Band Number
30 m - Blue	0.45 - 0.52	**Band 1**
30 m - Green	0.52 - 0.60	**Band 2**
30 m - Red	0.63 - 0.69	**Band 3**
30 m - Near Infrared	0.77 – 0.90	**Band 4**
30 m – Short-wave Infrared	1.55 - 1.75	**Band 5**
120 m – Thermal Infrared	10.40 – 12.50	**Band 6**
30 m – Shortwave Infrared	2.09 – 2.35	**Band 7**

Table 1: Properties of Landsat 4-5 TM

Landsat 8 OLI & TIRS Bands		
Spatial Resolution	Wavelength (micrometers)	Band Number
30 m - Coastal/Aerosol	0.435 – 0.451	Band 1
30 m - Blue	0.452 – 0.512	Band 2
30 m - Green	0.533 – 0.590	Band 3
30 m - Red	0.636 – 0.673	Band 4
30 m - NIR	0.851 – 0.879	Band 5
30 m - SWIR-1	1.566 – 1.651	Band 6
100 m - TIR-1	10.60 – 11.19	Band 10
100 m - TIR-2	11.50 – 12.51	Band 11
30 m - SWIR-2	2.107 – 2.294	Band 7
15 m - Pan	0.503 – 0.676	Band 8
30 m - Cirrus	1.363 – 1.384	Band 9

Table 2: Properties of Landsat 8 OLI & TIRS

Sensor	**Date**	**Path**	**Row**
Landsat 5 TM	2 March 1999	180	31
Landsat 5 TM	3 May 2010	180	31
Landsat 8 OLI & TIRS	25 March 2019	180	31

Table 3: Landsat images used in this study

3. METHODOLOY

3.1 Conversion of Digital Numbers to at-Sensor Radiance

The thermal data in satellite imagery of Landsat sensors are stored in Digital Numbers (DN). The pixels which are represented by DN values have not been calibrated into meaningful units. Thus, after acquiring the satellite images, digital numbers must be converted to radiance to have meaningful units (Ndossi and Avdan, 2016). In case of using Landsat 8 TIRS images, the following equation specifies the conversion of DN values to spectral radiance (USGS, 2018):

$$L_\lambda = M_L * Q_{cal} + A_L \qquad (1)$$

where L_λ is the Top-of-Atmosphere (TOA) spectral radiance in $W/m^2 * sr * \mu m$, M_L is the band specific multiplicative rescaling factor obtained from the metadata, A_L is the band-specific additive rescaling factor obtained from the metadata, Q_{cal} is the quantized and calibrated standard product pixel values (DN). Landsat 8 TIRS has two Thermal Infrared (TIR) bands which are band 10 and band 11. However, only band 10 is useful for LST retrieval at present due to uncertainties in band 11 (USGS,2018). Band-specific multiplicative rescaling factor (M_L), additive rescaling factor (A_L) and band specific thermal conversion constants (K1 and K2) that were used to calculate the at-sensor radiance were obtained from the metadata file of Landsat 8 image are shown in (Table 4).

Thermal Constant	**Band 10**	**Rescaling Factor**	**Band 10**
K1	1321.08	**M_L**	0.000342
K2	777.89	**A_L**	0.1

Table 4: Thermal constants and rescaling factors of the Band 10 of Landsat 8 image

For converting DNs to radiance while working with Landsat 5 TM and Landsat 7 ETM+ data, two equations are available. For this purpose, 'gain and bias' method and the spectral radiance scaling method can be used. Nevertheless, the spectral radiance scaling method is another representation of the gain and bias equation (Ndossi and Avdan, 2016). These two equations are shown in equations (2) and (3) respectively:

$$L_\lambda = gain * Qcal + bias \quad (2)$$

$$L_\lambda = ((LMAX_\lambda - LMIN_\lambda) / (QCALMAX - QCALMIN)) * (QCAL - QCALMIN)) + LMIN_\lambda \quad (3)$$

where L_λ = spectral radiance at the sensor's aperture in $W/m^2*sr*\mu m$,
gain = the rescaled gain $W/m^2*sr*\mu m$,
bias = the rescaled bias in $W/m^2*srad*\mu m$
Q_{CAL} = the quantized calibrated pixel value in DN
$LMIN_\lambda$ = the spectral radiance that is scaled to QCALMIN in $W/m^2*sr*\mu m$
$LMAX_\lambda$ = the spectral radiance that is scaled to QCALMAX in $W/m^2*sr*\mu m$
QCALMIN = the minimum quantized calibrated pixel value and
QCALMAX = the maximum quantized calibrated pixel value

3.2 Brightness Temperature Calculation

Temperature measurements can be represented by the brightness temperature. However, it lacks to represent the physical meaning of temperature (Wang, 2012 as cited in Ndossi and Avdan, 2016). After the conversion of digital numbers to radiance, the radiance must be converted to brightness temperature. In order to do this, following equation is used (USGS, 2018):

$$Tsen = \frac{K_2}{ln\left(\frac{K_1}{L\lambda}+1\right)} \quad (4)$$

Where
Tsen = at-sensor brightness temperature (K)
Lλ = TOA spectral radiance
K1 = band specific thermal conversion constant from the metadata
K2 = band specific thermal conversion constant from the metadata
The same equation is used for all sensors. The K1 and K2 values may vary depending on the sensor and the wavelengths by which the thermal bands operate. The values of K1 and K2 can be obtained from the metadata file of a scene (Ndossi and Avdan, 2016).

3.3 Estimation of Land Surface Emissivity (LSE)

It is necessary to do LSE correction while deriving LST from space. The emissivity of different terrestrial materials can be estimated by the use of Normalized Difference Vegetation Index (NDVI) in 10-12 μm wavelength range (Wang, 2015 as cited in Ndossi and Avdan, 2016). Since the properties of the land surface changes with time, it is important to determine the LSE of an area in the satellite overpass time (Ndossi and Avdan, 2016). Therefore, NDVI calculation is possible by the use of following formula:

$$NDVI = \frac{NIR-Red}{NIR+Red} \quad (5)$$

Where NIR is the near infrared band and red is the red band. After the calculation of the NDVI values, to estimate the emissivity value, the equation proposed initially by Sobrino et al. (2004) is used:

$$e = 0.004*Pv + 0.986 \quad (6)$$

Where:

e = land surface emissivity from NDVI;

P*v* = Proportion of vegetation

Proportion of vegetation can be obtained by the following formula:

$$Pv = \left[\frac{NDVI-NDVImin}{NDVImax-NDVImin}\right]^2 \quad (7)$$

Where:

NDVI = Normalized Difference Vegetation Index
NDVI min = minimum value of NDVI
NDVI max = maximum value of NDVI
The atmospheric correction of the NIR and red bands was made in QGIS environment for calculating the NDVI. NDVI images on 1999, 2010 and 2019 were shown in Figure 2 , 3 and 4.

Figure 2: NDVI image March 3, 1999

Figure 3: NDVI image May 3, 2010

Figure 4: NDVI image March 25, 2019

3.5 Brightness Temperature Emissivity/ Atmospheric Correction

The correction of brightness temperature against LSE and atmospheric parameters is important. There are various algorithms for estimating LST from thermal infrared satellite imagery. These algorithms have their own limitations and differences in level of accuracies and varies from one sensor to another (Ndossi and Avdan, 2016). In this study, inversion of Planck's function is used (Artis and Carnahan, 1982 as cited in Ndossi and Aydan, 2016). It corrects the emission of a substance in comparison to a blackbody.

$$Ts = \frac{BT}{1+\left(\frac{\lambda \cdot BT}{\rho}\right) \cdot ln\varepsilon} \qquad (8)$$

Where Ts is the land surface temperature (K), BT is the at- sensor brightness temperature, $\boldsymbol{\lambda}$ is the wavelength of the emitted radiance, $\boldsymbol{\rho}$ is $1.438.10^{-2}$ mK and $\boldsymbol{\varepsilon}$ is the spectral emissivity

4. RESULTS and DISCUSSION

According to United Nations population data 52.1 % of world population, corresponding 3.6 billion people were living in urban areas in 2011 (United Nations, 2012). So, urbanization and human activities such as industry, commerce, energy consumption, water use, landscaping area and other environmental and social correlations play an important role in developing world since these issues affect wide range of areas. Therefore, issues influenced by these factors should also be investigated. In this aspect, urbanization and industrialization especially seen in big cities, cause environmental pollution. This situation has led to an increase in air temperatures on global scale, thereby the environment and human health have become damaged. Therefore, determination of surface temperatures has become a very important issue both for the protection of human and environmental health and for the future of the cities. In this context, remote sensing has become a prominent method in determination of surface temperatures in recent years. In this study, LST maps of Istanbul of different times have been obtained by the use of Landsat 5 TM and Landsat 8 OLI & TIRS images. LST has been estimated by the use of Planck's function. LSE estimation of the study area has been done by the use of equation initially proposed by Sobrino et al. (2004).

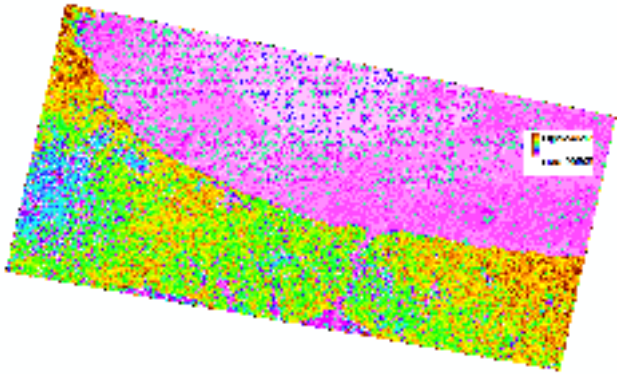

Figure 5: Land surface temperature image of Istanbul March 3, 1999

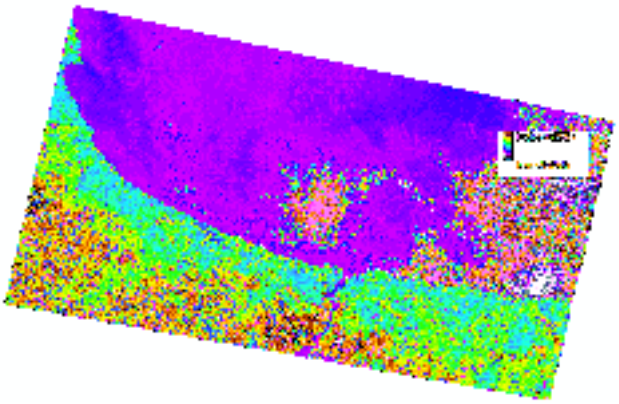

Figure 6: Land surface temperature image of Istanbul May 3, 2010

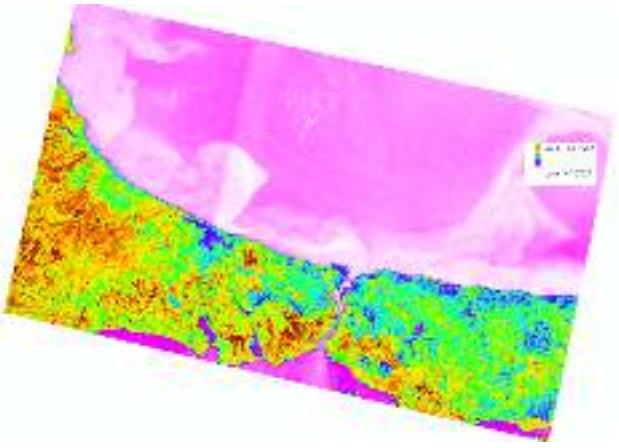

Figure 7: Land surface temperature image of Istanbul March 25, 2019

Figures 5 and 6 show the LST maps produced by Landsat 5 imagery dated March 3, 1999 and May 3, 2010. Figure 7 shows the LST map produced by the Landsat 8 OLI & TIRS imagery dated March 25, 2019. The satellite images which are acquired on the same season have been chosen to obtain meaningful results in order to

compare the temperatures. The images acquired on the spring season were used in the study. The atmospheric factors, especially the cloud cover presence is one important factor for land surface temperature estimation. However, the land surface on the selected images has not been affected by the cloud cover. The satellite images used in the study were selected which have cloud cover of less than 10%. The land cloud cover of the images is 3% in 1999, 1% in 2010 and 0.06% in 2019 respectively. Therefore, no mask is applied for clouds during the case study.

According to the study of Geymen and Baz (2007), between 1990 and 2005, the distribution of the settlements to total area has increased from 11% to 16% and the distribution of agricultural areas has decreased from 27% to 23%. On the other hand, according to Turkish Statistical Institute (TSI) data, the population density (people per square kilometer) of İstanbul was 2900 in 2018 while it was 2420 in 2007.

Unplanned urbanization and distorted construction caused by this situation have changed the building stock in the study area significantly. Thus, the surface temperature was affected by this rapid increase in building stock and population. The results obtained in this context show that, a rapid temperature increase is observed in the study area between 1999 and 2019. Minimum and maximum values of the temperature during the period between March 1999 and March 2019, clearly indicates the temperature change in the specific month over 20 years. In addition, bare lands and reinforced concrete structures stand out as the highest surface temperature values in the study area, whereas the areas covered with forest and vegetation have the lowest land surface temperature.

It has been observed that the decrease in the amount of areas covered with vegetation and water between 1999 and 2019, which can be detected from the satellite images, plays an important role on the increase of the surface temperature.

The importance of green areas for development and the future of cities were once again demonstrated by this study. Therefore, it can be said that the management of the green areas should be well planned in the future to prevent the rapid increase of the temperature in the study area.

The effects of vegetated regions on surface temperature which this study indicates should be taken into consideration while planning construction studies. On the other hand, it can be said that in case of periodically producing; land surface temperature maps can be used in different studies such as regional climate changes etc.

5. ACKNOWLEDGMENTS

The authors would like to thank USGS/Earth Explorer for providing freely Landsat 8 OLI & TIRs and Landsat 5 TM data.

REFERENCES

Artis, D.A.& Carnahan, W.H. Survey of emissivity variability in thermography of urban areas. Remote Sensing of Environment 1982, 12, 313–329.

Geymen, A & Baz, İ. (2007). İstanbul Metropolitan Alanındaki Arazi Kullanım Değişimi ve Nüfus Artışının İzlenmesi. HKMO Ulusal CBS Kongresi 30 Ekim–2 Kasım 2007, KTÜ, Trabzon

Google Earth. (2019). Turkey. 40˚58'N 28˚50'E [10.03.2019]

Jeevalakshmi, D & Narayana Reddy, S & Manikiam, Balakrishnan. (2017). Land surface temperature retrieval from LANDSAT data using emissivity estimation. International Journal of Applied Engineering Research. 12. 9679-9687.

Landsat Science. (2019). *Landsat 8.* Retrieved from https://landsat.gsfc.nasa.gov/landsat-8/ [20.03.2019]

Li, Zhao-Liang & Duan, Si-Bo. (2017). Land Surface Temperature. 10.1016/B978-0-12-409548-9.10375-6.

Lv, Z & Zhou, Q. (2011). Utility of Landsat Image in the Study of Land Cover and Land Surface Temperature Change, Procedia Environmental Sciences, Volume 10, Part B Pages 1287-1292, ISSN 1878-0296, https://doi.org/10.1016/j.proenv.2011.09.206.

Ndossi,M;I & Avdan, U. Application of Open Source Coding Technologies in the Production of Land Surface Temperature (LST) Maps from Landsat: A PyQGIS Plugin.*Remote Sens.*2016, *8*, 413.

Sobrino, Jose & Jimenez-Munoz, Juan-Carlos & Paolini, Leo. (2004). Land surface temperature retrieval from LANDSAT TM 5. Remote Sensing of Environment. 90. 434-440. 10.1016/j.rse.2004.02.003.

Turkish Statistical Institute. (n.d). *Yıllara göre illerin yıllık nüfus artış hızı ve nüfus yoğunluğu, 2007-2018.* Retrieved from www.tuik.gov.tr/Tablo.do?istab_id=1591.[15.4.2019]

United Nations (2012). Department of Economic and Social Affairs, Population Division, World Urbanization Prospects.

U.S. Geological Survey. (n.d.). *Landsat 5*. Retrieved from https://www.usgs.gov/land-resources/nli/landsat/landsat-5 [20.03.2019]

U.S. Geological Survey. (2018). *Landsat 8 Data Users Handbook*. Retrieved from https://prd-wret.s3-us-west-2.amazonaws.com/assets/palladium/production/s3fspublic/atoms/files/LSDS-1574_L8_Data_Users_Handbook.pdf [20.3.2019]

Wang, F.; Qin, Z.; Song, C.; Tu, L.; Karnieli, A.; Zhao, S. An improved mono-window algorithm for land surface temperature retrieval from Landsat 8. Remote Sens. 2015, 7, 4268–4289.

Wang, S.L.L. Chapter 8—Land-surface temperature and thermal infrared emissivity. In Advanced Remote Sensing; Wang, S.L.L., Ed.; Academic Press: Boston, USA, 2012; pp. 235–2